Snow cover investigations by means of ERS-SAR imagery on the Antarctic Peninsula

C. Schneider, S. Wunderle, M. Friedrich

Department of Physical Geography, University of Freiburg
Werderring 4, D-79085 Freiburg, Germany
e-mail: chri@ipg.uni-freiburg.de

Abstract

The west coast of the Antarctic Peninsula (AP) is an area of extraordinary sensitivity in respect to climate change. However, sparse meteorological data hampers the assessment of regional climate trends. The mountain chain of the AP covers a wide range of climates, because of its large extension from north to south. Consequently, regional circulation pattern and latitudinal and hypsometric temperature gradients lead to spatial differentiation of the types of the permanent snow cover. Climate variations influence the distribution of dry snow zone, percolation zone and wet snow zone. Therefore, changes of the spatial pattern of these snow zones can be attributed to regional climate change.

Investigations into snow cover dynamics of the AP greatly benefit from the utilisation of space-borne SAR imagery. SAR images provide insight into the snow cover not only locally but as spatially distributed data. SAR data are characterised by the all-weather capability of the system and its ability to receive information from deeper layers of the snow pack. The backscatter signal obtains contributions from the snow volume and from scattering at the surface and from scattering at surfaces of internal strata. Profound knowledge of the terms dominating the backscatter signal is a prerequisite to extract relevant information. On snow surfaces with predominant surface scattering the signal strongly varies with exposition, slope and surface roughness. Volume scattering is mainly influenced by grain size, stratification and by liquid water content in the snow cover. These parameters reflect recent and actual meteorological conditions. Hence, meteorological measurements to estimate the state of the snow cover in terms of temperature distribution and energy budget substantially back the interpretation of the SAR image. In this study we propose a new application of data from space-borne microwave systems in the field of climatology. A simple energy budget model is used to derive the location of the transition from dry to wet snow using data from automatic weather stations and a digital elevation model for two glaciers in Marguerite Bay at 68° south. Vice versa, SAR imagery can contribute spatial information of the snow cover to meteorological and hydrological point measurements because SAR imagery enables to delineate areas with differing snow types. Results obtained from both methods are consistent. We use these relations to propose a monitoring scheme to assist climate monitoring in the western Antarctic Peninsula region.

1. INTRODUCTION

1.1. Study area

The Antarctic Peninsula (AP) (fig. 1) expands over a wide range of sub-polar and polar climates (King and Turner 1997). In conjunction with southern South America the mountain range of the AP acts as the only major barrier to the westward circulation associated with the circumpolar low pressure trough in the southern hemisphere (Schwerdtfeger 1984). The AP comprises a glaciated landscape with a large variety of different glacial systems such as ice sheets, ice caps, outlet glaciers, alpine type valley glaciers, fringing glaciers, permanent firn and ice shelves (Fleming *et al.* 1938, Wyeth 1977, Doake 1982). The spatial pattern of the landscape is complicated, on account of huge differences in air temperature and precipitation, both from north to south and from west to east (Reynolds 1981, Peel 1992a), on account of variations related to local climate phenomena (Schwerdtfeger 1984) and on account of orographic effects (Morris and Vaughan 1994).

The peculiar topographic and climatological situation on the AP is attracting much interest in respect to global change scenarios. Although global circulation models (GCM) do not predict extraordinary warming rates when compared to other marginal zones of the Antarctic continent (Houghton 1996), recently much evidence of climate change in the last decades has been gathered by different authors. The west coast of the AP shows extreme year to year variability in respect to air temperature, which is mainly attributed to fluctuations in sea-ice extent (King 1994). A significant warming trend of +5.5°C in mid-winter and +1.5°C in summer was determined by Smith and Stammerjohn (1996) for the time period from 1941 to 1991. Reduction, and even decay of ice shelves, has been reported by different authors (Doake and Vaughan 1991, Skvarca 1993, Rott

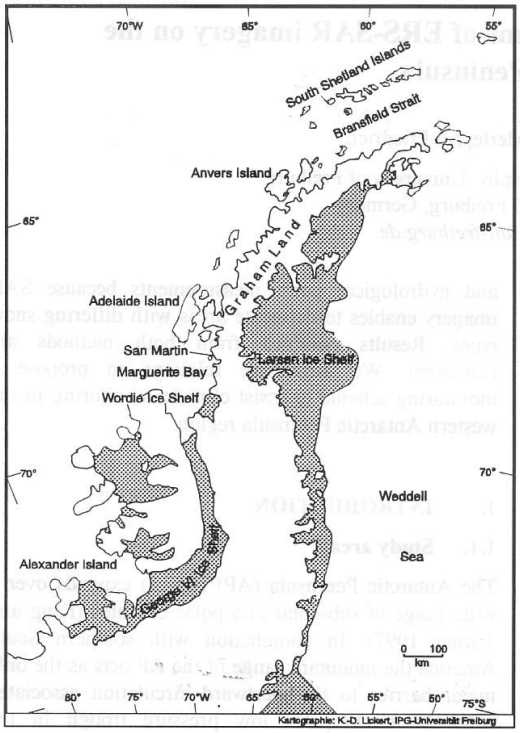

Fig. 1: Map of the Antarctic Peninsula. The area of investigation is located in the vicinity of the Argentine Research Base 'San Martin'.

et al. 1996). This corresponds to a shift of the -5°C mean annual isotherm to the south by approximately 200 km on the west coast and 50 km on the east coast of the AP (Vaughan 1993, Vaughan and Doake 1996). Annual precipitation rates have increased by 20% since 1950 according to Peel (1992a).

We have selected two glaciers at 68° south in Marguerite Bay for detailed studies. Marguerite Bay area is a region of pronounced environmental change due to atmospheric warming trends in recent years (Smith and Stammerjohn 1996). Especially during the winter Marguerite Bay marks the transition from sub-polar maritime climate to polar climate with continental attributes (Harangozo *et al.* 1997). The observed environmental change influences spatial extent and distribution of snow zones. Since the response time of glaciers may be in the order of decades information from the snow cover can help to investigate climate variability within shorter periods of time.

1.2. Snow zones and local climate

The extension and the location of different snow zones are closely linked to local climate and actual weather. The actual weather situation and the meteorology during the time period before image acquisition specifically transform the snow or firn. All major snow zones as discussed in Paterson (1994) can be found on the AP.

The zone of permanent dry snow is restricted to areas where air temperature is permanently below 0°C. These regions are roughly coincident with areas below -11°C of mean annual air temperature (Peel 1992b) on the plateau of the AP in southern Graham Land and in Palmer Land. The intermediate snow zone, where melting occurs occasionally is called the percolation zone. Enhanced growth of snow grains, accentuated stratification and further densification of the snow in comparison to the dry snow zone can be observed in the percolation zone. In summer the wet snow zone develops on the lower reaches of most valley glaciers along the west coast of the AP and on the ice caps to the north of the AP. Recent energy exchange with atmosphere and actual temperature level define the occurrence of melting in the snow pack. Therefore, location of the transition from actual wet snow zone to actual dry snow zone depends on recent weather conditions. This relation is exploited in section 4. The actual extent of the wet snow zone is derived from an energy budget model using data from an automatic weather station and a digital elevation model (DTM). Hence, inter-annual variations of mean wet snow extent in summer can be attributed to variations of regional climate. The combination of distinct snow cover properties leads to characteristic radar backscatter. Nevertheless different combinations of factors may result in similar backscatter values. Therefore ground truth campaigns focus on sampling information on relevant key parameters. Combining ground truth data and altitudinal information derived from DTMs with the theoretical approaches described in section 2, spatial extent of snow zones can be extracted precisely from SAR data (see section 3). Climate trends may be revealed from multi-year time series of SAR data, because distinct shifts of snow zones can be related to climate fluctuations.

2. BACKSCATTER THEORY

Both passive and active microwave satellite data are used widely for studies on snow properties (e.g. Ulaby *et al.* 1982, Hallikainen 1996, Mätzler 1987, West 1996). The all-weather capability of these systems allows to obtain data on a reliable basis. Polar night does not impose problems in respect to image acquisition. The signal from the ground is partly composed of contributions from the surface and from the volume of the snow pack. This opens excellent possibilities for investigations of the snow cover in climatology and glaciology in addition to optical and thermal remote sensing data. Passive microwave data is used widely in Antarctica in respect to sea ice extent

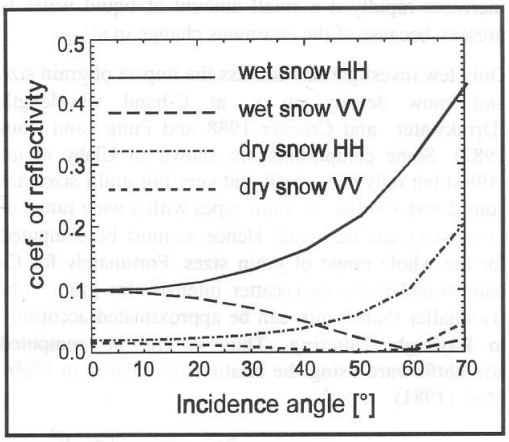

Fig. 2: Coefficient of reflectivity (Γ) at 5.3 GHz as modelled for dry snow with a snow density of 0.35 g/cm^3 and wet snow with 12% liquid water content and a snow density of 0.45 g/cm^3 for vertical and horizontal polarisation.

(Stammerjohn and Smith 1996, Zwally *et al.* 1983) and monitoring of large-scale surface melting (Zwally and Fiegles 1994). The emission of radiative energy from the snow pack at microwave frequencies however is small in comparison to the backscatter intensity obtained by active systems. Consequently spatial resolution of space-borne passive microwave sensors is poor. Zwally and Fiegles (1994) give an effective pixel size of 3.000 km^2 for the SMMR (Scanning Multichannel Microwave Radiometer) of the Nimbus-7 satellite. Therefore, passive microwave data can only be used at meso- and macro-scale levels. Studies addressing snow cover dynamics by means of spaceborne sensors on a regional scale must make use of active microwave data with a pixel resolution of at least a few decametres. Hence, in respect to studies on regional climate variability on the AP, we concentrate on the interpretation of active microwave data, especially on data from the ERS-1 and ERS-2 synthetic aperture radar (SAR). This data however are restricted in terms of temporal coverage. Repeat time is up to 35 days depending on satellite orbit and location. Also, the limited operation of the receiving station on the AP is a limiting factor. Utilisation of data of the Canadian RADARSAT system may offer new possibilities because of the possible variations in incidence angle and polarisation.

Since a part of the backscatter signal comes from the snow volume, properties such as liquid water content, grain size, shape and orientation of snow crystals, snow density and ice lenses influence the backscatter signal. Fig. 4: Snow profile from 03.02.1995, McClary Glacier. Black layers stand for ice lens in respect to surface scattering, surface roughness and local incidence angle have to be considered. The underlying ground also contributes to the signal if the radiation penetrates the snow pack completely. In order to identify the most important snow cover properties the physics of backscatter behaviour have to be outlined. The power received by the SAR is given by (Ulaby 1982): with P_r the received power, λ the wave length, P_t the transmitted power, G the antenna gain, A the illuminated surface area, R the distance from the antenna to the ground and σ^0 the back-scattering coefficient. σ^0 summarises all effects that result from geometry and dielectric characteristics of the target area. σ^0 is composed of scattering at the surface (σ^0_s) and of volume scattering (σ^0_v).

2.1 Dielectric constant

The complex dielectric constant (ε) of snow, which can be regarded as a mixture of ice crystals, air and water, is given by:

$$\varepsilon = \varepsilon' - i\varepsilon'' . \qquad (2)$$

At the fixed frequency of 5.3 Ghz of the ERS ε can be approximated from snow density and liquid water content (Tiuri *et al.* 1984, Mätzler 1987, Ulaby *et al.* 1986). ε of dry snow varies from ε_{ds}=1.4-i*0.0002 for snow with a density of 250 kg/m^3 to ε_{ds}=2.3-i*0.0009 for snow with a density of 600 kg/m^3. Liquid water in the snow severely changes the dielectric properties because ε and especially ε'' of water is very high at 5.3 Ghz. For snow with a density of 500 kg/m^3 we obtain:

ε_{ds} = 1.9 - i*0.0007 0% liquid water content,
ε_{ws} = 2.1 - i*0.1 2% liquid water content,
ε_{ws} = 4 - i*0.8 12% liquid water content.

2.2 Surface scattering

σ^0_s is a function of incidence angle (θ), coefficient of reflectivity (Γ) and surface roughness. Γ depends on the difference of the complex dielectric constant (ε) of the two media which define the boundary. Γ is smaller than 0.05 at the boundary from dry snow to air. ε of wet snow, in particular its imagery part, is much higher (Mätzler 1987). Γ of wet snow is as high has 0.15. Fig. 2 shows the dependency of Γ from incidence angle for wet and for dry snow at different polarisations. For vertical polarisation Γ is computed according to

$$\Gamma_{\parallel} = \left| \frac{\eta_1 \cos\theta_1 - \eta_2 \cos\theta_2}{\eta_1 \cos\theta_1 + \eta_2 \cos\theta_2} \right|^2 \qquad (3)$$

given by Ulaby *et al.* (1981). The magnetic

permeability η is related to ε by

$$\eta = \sqrt{\frac{\mu_r}{\varepsilon_r}} \approx \sqrt{\frac{1}{\varepsilon_r}}. \quad (4)$$

At small incidence angles Γ is mainly depending on the snow type. The decrease of Γ for vertical polarisation at about $\theta \approx 60°$ is caused by the Brewster angle, where no reflection is observed at all.

Incidence angle and surface roughness together define the angular pattern of σ^0_s. Backscatter near nadir is very high in comparison to higher values of θ. Smooth surfaces give strong σ^0_s at nadir but σ^0_s decreases rapidly with increasing θ. Rough surfaces show moderate backscatter at $\theta \approx 0°$ but this decreases less pronounced at higher incidence angles. Details are given in Ulaby *et al.* (1986). Stationary-Phase Approximation was used to compute σ^0_s for rough surfaces (Ulaby 1986). Scalar Approximation as presented in Drinkwater (1989) was employed to model backscatter from smooth surfaces. Calculations for σ^0_s for dry snow surfaces with the parameters of the antenna of the ERS-SAR system (λ=5.6 cm, $\theta \approx 22°$ and vertical polarisation) showed very low backscatter contribution of the surface. σ^0_s was smaller than -20dB for all roughness scales. In accordance with Ulaby (1982) and Fung and Chen (1989) it is concluded that surface scattering can be neglected for dry snow because of the low coefficient of reflection. In case of wet snow and high reflectivity σ^0_s ranges from 0dB to -20dB, strongly depending on liquid water content, incidence angle and surface roughness. σ^0 for wet snow can be dominated by contribution from surface scattering.

2.3. Volume scattering:

Radiation penetrating media is weakened due to absorption in the volume and scattering at inhomogeneties. These losses are described by the absorption coefficient κ_a and the scattering coefficient κ_s. Both are related to the extinction coefficient (κ_e) with

$$\kappa_e = \kappa_a + \kappa_s. \quad (5)$$

The penetration depth δ_p of microwaves into media can be calculated by:

$$\delta_p = 1/\kappa_e. \quad (6)$$

The absorption coefficient is related to the quotient of the imaginary and the real part of the dielectric constant (Hallikainen and Ulaby 1986):

$$\kappa_a = \frac{2\pi}{\lambda}\sqrt{\frac{1}{2}\left(\sqrt{1+\left(\frac{\varepsilon''}{\varepsilon'}\right)^2} - 1\right)} \quad (7)$$

Consequently absorption is low for dry snow and increases rapidly if a small amount of liquid water is present, because of the enormous change in ε''.

Only few investigations address the impact of grain size and snow density on κ_s at C-band wavelength (Drinkwater and Crocker 1988 and Fung and Eom 1982). Some computings are shown in Ulaby *et al.* (1986) but only very small and very big grain sizes are considered. On the AP snow types with a wide range of grain sizes can be found. Hence κ_s must be computed for the whole range of grain sizes. Fortunately for C-band wavelengths backscatter intensity for grain radii (r) smaller than 5 mm can be approximated according to Rayleigh scattering. Thus κ_s can be computed straightforward using the relation formulated in Ulaby *et al.* (1981)

$$\kappa_s = \tfrac{2}{3}\sigma_v = \frac{2}{3}\frac{64*\pi^5*r^6}{\lambda^4}*(\varepsilon')^2*\left|\frac{\varepsilon-1}{\varepsilon+1}\right|^2*N_r \quad (8)$$

with N_r the number of snow crystals per m³.

Figure 3 shows the increase of the scattering coefficient with increasing grain size. The impact of snow density is not as pronounced. The maximum variation of κ_s in respect to snow density yields a factor of 10. However, κ_s rises by a factor of 100 if grain radius is changed from 0.5 mm to 3 mm. Application of scattering theory to snow packs often results in complicated approaches (West *et al.* 1993, Chuah *et al.* 1997). Parameters used in these models such as crystal shape and crystal orientation are difficult to obtain in the field (Rott 1984). For dry snow an approximation of σ^0 only based on snow density, stratification and grain size can be obtained employing the backscatter model presented in Ulaby *et al.* (1982) (9):

$$\sigma^0_{pack}(\theta) = (1-\Gamma(\theta))^2 * \left(\sigma^0_{ds}(\theta') + \frac{\sigma^0_{soil}(\theta')}{L^2(\theta')}\right) \quad (9)$$

with:

θ': angle of refraction in snow obtained from Snell's law

$\mathbf{L}(\theta') = \exp(\kappa_e * \mathbf{d} * \sec(\theta'))$: one-way loss factor of a snow layer

d: thickness of snow layer

$\sigma^0_{soil}(\theta')$: backscatter of underlying soil surface or glacier ice.

The backscatter from a single snow layer ($\sigma^0_{ds}(\theta')$) is given by,

$$\sigma^0_{ds}(\theta') = \frac{\sigma_v * \cos(\theta')}{2*\kappa_e}\left(1 - \frac{1}{L^2(\theta')}\right) \quad (10)$$

with

with $\sigma_v = 1.5 * \kappa_s$ (11)

Computation of backscatter from a dry snow pack for C-band with this approach returns comparable results to the data cited in Jezek *et al.* (1993). The only parameters that have to be known are the vertical pattern of snow density and grain size. Snow density is used to compute ε. Any multilayer snow pack can be computed by iterative application. For every single layer σ^0 is calculated by taking the next layer further down as σ^0_{soil} and calculating L(θ) for all overlying layers together. σ^0_s, of surfaces of internal strata is computed according to the Scalar Approximation and added to the total backscatter. Backscatter from the volume of depth hoar layers is estimated using data sampled by Reber *et al.* (1987) for X-band with further adjustment in respect to the different wavelength of the ERS-SAR system.

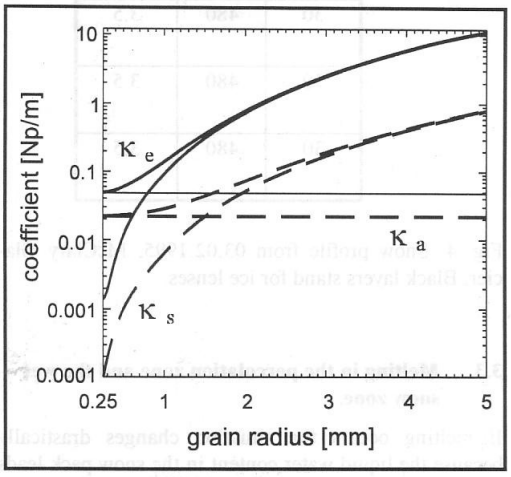

Fig. 3: Coefficients of extinction (κ_e), absorption (κ_a) and scattering (κ_s) at 5.3 GHz for dry snow with a snow density of 0.25 g/cm^3 (dotted line) and 0.65 g/cm^3 (solid line) as a function of grain radius.

3. BACKSCATTER INTENSITY FROM DIFFERENT SNOW TYPES

3.1 Dry snow zone

The dry snow zone appears on the AP at high elevations on the plateau. The only process in the snow pack is slow metamorphism by densification of the firn by overlying snow and the formation of wind crusts. These areas show very low values of σ^0, between -15dB and -20dB, in ERS-SAR images (Wunderle 1996a). Since there is no contribution from liquid water or ice lenses to the backscatter intensity we can use the model to estimate snow density and grain size. Assuming a 4 m top layer with a density of 350 kg/m³ and grain radius of 0.5 mm and a metamorphosed deeper layer with 1 m thickness, density 450 kg/m³ and grain radius of 1 mm we obtain a backscatter coefficient of $\sigma^0(22°)$=-12dB. The largest portion is the contribution of the deeper layer, because the extinction within the top layer is very weak due to the small grain size. With a grain radius of 0.75 mm for the bottom layer $\sigma^0(22°)$ decreases to -17dB. This value corresponds to the values found in the SAR image. Thus, modelling shows that metamorphism in the dry snow zone of the plateau of Palmer Land is not able to increase snow grain radii to values larger than r=0.75 mm.

The applied backscatter model is compared to ground truth data and scatterometer measurements presented in Rott *et al.* (1993). Although no grain size is indicated it is possible to estimate the contribution of volume scattering for a sample site in the dry snow zone with 8 depth hoar layers and a snow density of 450 kg/m^3 at 1200 m asl in Dronning Maud Land (74° south, 13° west). At the Brewster angle where no surface scattering occurs Rott *et al.* (1993) cite a value of -18 dB at C-band. This is used to derive a mean value for r of 0.75 mm. Firn cores gathered by the German Alfred-Wegener-Institut in the same area showed similar grain sizes (Oerter 1997, personal communication). From the iterative application of the model to a snow pack with the observed properties $\sigma^0(10°) \approx$-7dB was obtained. This is in fair agreement with the result of the scatterometer measurements of $\sigma^0(10°) \approx$-5dB presented in Rott *et al.* (1993). The large difference between backscatter intensity at small incidence angle and at Brewster angle can only be explained by the contribution from the surface scattering at internal strata at all boundaries in the snow pack, because volume scattering shows no dependency of incidence angle. This indicates that the impact of series of ice lenses and depth hoar layers to σ^0 is strong for dry snow with small grain size as also suggested by (Rott *et al.* 1993). Calculation for the incidence angle of ERS-SAR (22°) yields -13dB, signifying the importance of local incidence angle in respect to surface scattering.

3.2. Frozen percolation zone.

The percolation zone shows occasional melting at the surface during the summer season with liquid water and extensive metamorphosis in the snow cover. Large rounded crystals and ice lenses result from melting. Formation of depth hoar can be observed when the water vapour gradient is directed upwards in the snow pack. In this section we discuss the winter situation without any liquid water content. The contribution to the backscatter intensity from ice lenses is computed according to the Scalar Approximation. We find that due to the small change of ε between ice and dry snow within the snow

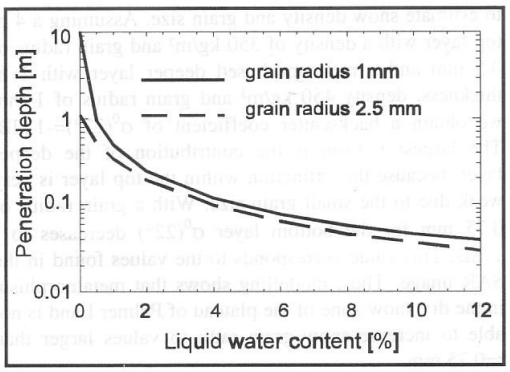

Fig. 5: Penetration depth for different grain radii as a function of liquid water content.

according to the Scalar Approximation. We find that due to the small change of ε between ice and dry snow within the snow pack the reflectivity and the contribution of surface scattering to the total backscatter intensity is small. Depending on snow density and θ computations provide:

$$0.005<\Gamma<0.03 \qquad (12).$$

A snow profile (Fig. 4) from February 3rd 1995 on the McGlary Glacier at 550 m asl was selected to model the backscatter intensity the satellite would receive. In winter in the absence of any melt water the area appears bright in the ERS-SAR image with $\sigma^0(22°)\approx$-4dB (Wunderle 1996b). Grain radii ranged from 0.75 to 2 mm. Snow layers were separated by thin ice crusts. The accumulative backscatter from all snow layers was computed to -6.8 dB. Contribution of surface scattering at ice lenses in the pack at an incidence angle of 22° increases σ^0 to -6.0 dB. Integration of volume scattering from the ice crusts ice lenses further rises this to -5.2 dB. This is in good agreement with the value found in the ERS-SAR winter image. The small difference between calculations with and without the contribution from the internal surfaces indicates that the internal stratification of a snow pack with large grain radii is not important. σ^0 is dominated by volume scattering.

A similar interpretation can be deduced from the scatterometer measurements presented in Rott *et al.* (1993). For a sample site in the percolation zone in Dronning Maud Land at 500 m asl the backscatter intensity of 0dB at 10° incidence angle is only reduced to -4dB at the Brewster angle of 60°. Backscatter intensity from snow with large grains below 0°C is so intense, that the contribution of ice lenses compared is of minor importance.

Height [10^{-2} m]	Density [kg/m^3]	Diameter [10^{-3} m]
14	220	1.5
15	475	2
11	475	2.5
26	475	2.5
8	520	2.5
13	520	2.5
19	520	2.5
8	450	3
17	450	3.5
5	480	3
15	480	3.5
15	480	3.5
30	480	3.5
30	480	3.5
30	480	3.5

Fig. 4: Snow profile from 03.02.1995, McClary Glacier. Black layers stand for ice lenses.

3.3. Melting in the percolation zone and the wet snow zone.

If melting occurs the situation changes drastically because the liquid water content in the snow pack leads to strong absorption. As a consequence, σ^0 for wet snow is much smaller than for dry snow (Ulaby *et al.* 1986, Mätzler 1987, Drinkwater 1989). The dramatic reduction of δ_p is shown in fig. 5. Since σ_v is not significantly higher for wet snow in comparison to dry snow, the total contribution of volume scattering to σ^0 is much smaller because the volume is reduced. δ_p would be reduced to 0.2 m assuming 2% of liquid water content in the profile in fig. 4. Then σ_v can only be calculated from the two upper most layers and is approximately -20dB. ERS-SAR data from this area show values from -20dB to -14dB in summer (Wunderle 1996b). The variation is due to a changing amount of liquid water in the snow and varying surface roughness and surface inclination.

4. APPLICATION IN CLIMATOLOGY

Remote sensing contributes spatially distributed information to the point meteorological time series. Parameters of the snow pack defined by meteorological conditions influence the backscatter intensity. This offers the possibility to monitor changes in the snow pack and the variability of climate elements on a seasonal and on an inter-annual time scale. We illustrate this using SAR data from two glaciers at 68° South in Marguerite Bay on the west coast of the AP. First we describe the SAR image and give some interpretation in respect to snow zones. Afterwards a model approach is shown to relate meteorological measurements and SAR imagery.

4.1. SAR image

The SAR image dating from 18th January 1995 (fig. 6b) depicts parts of Marguerite Bay at 68° south and 67° west. It is rectified according to the digital elevation model (DTM) of the area. The central parts of the image comprise the glaciers McClary - to the north - and Northeast - to the south. Both glaciers form a joined ice cliff, which faces west. Both ice streams are flanked by ridges with summits at altitudes between 700 and 1000 m asl. The ridges can be recognised from the layover in the image.

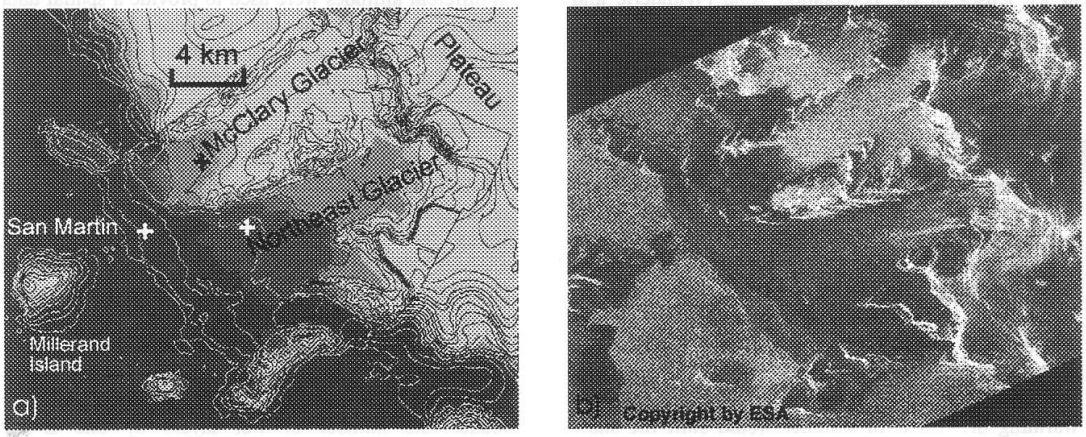

Fig. 6: Map of investigation area and model result for 18th January 1995. The upper left corner is located at 67°17'33'' west and 68°14'06'' south.
a) Model result for the time of image acquisition. Contour lines with 100m intervals derived from the DTM are overlaid. Discontinuities at contour lines result from merging DTMs with different resolution. The crosses mark the locations of AWS. All areas with shaded grey tones represent areas with some liquid water content leading to reduced backscatter intensities on the SAR image. Only the lightest grey tone stands for areas with absolutely frozen snow and with no liquid water content at all.

b) ERS-1 PRI image from 18th January 1995, 2:00 local time covering the same area as figure 6(a). Bright areas on the north-western parts of McClary Glacier belong to the percolation zone. The low-lying parts of McClary and the surface of Northeast Glacier are depicted in dark tones signifying the presence of liquid water in the wet snow zone. The dry snow on the plateau also leads to low backscatter intensity in the SAR image.

Snow zone	Example of location	Backscatter intensity on ERS-SAR scene	Dominant parameter
Dry snow zone	Plateau of Antarctic peninsula	-18 dB	Grain size, density
Percolation zone - frozen	McClary glacier (summer)	-4 dB	Grain size, ice lenses
Wet snow zone - frozen	Northeast glacier (winter)	-2 dB	Grain size ice lenses
Wet snow zone - melting	Northeast glacier (summer)	-19 dB	Liquid water content

Table 1: Mean backscatter derived from ERS-SAR scenes of the AP at 68° south. Northeast and McClary glacier are located on the west coast of the AP in Marguerite Bay.

The dark tone in the image on the glacier surface adjacent to the ice cliff is due to wet conditions in the snow cover. This leads to heavy absorption of the microwave radiation of the ERS. The extension of the wet snow zone is closely related to temperature and radiation. Therefore it is a good indicator for temporal variability of climate elements during the summer season. This relation is discussed in detail in the next section. Further to the east, at higher altitudes on the Mclary Glacier, the transition to lighter tones can be observed. Here, temperatures in the snow cover are well below zero and the absorption of the radiation decreases rapidly due to the total absence of liquid water in the snow cover. Consequently, the bright colour results from scattering at large snow grains and at ice lenses in the percolation zone (Wunderle and Saurer 1995). The right margin of the image shows surfaces in dark tones on the plateau at altitudes higher than 1000 m asl where air temperatures are below 0°C throughout the year (Wunderle 1996a). No distinct ice lenses and only small grain size can be observed there, because no metamorphosis from melting occurs here. Consequently, backscatter from these surfaces in the dry snow zone is much smaller compared to the percolation zone. When multi-year SAR data is available the shift of the altitude of the transition from percolation- to dry snow zone indicates climate variability in terms of positive extremes of air temperature. We expect that a warming trend would shift this transition to higher altitudes. With a lapse rate of 0.6°C/100m (Morris and Vaughan 1994) a warming of +1.8°C in summer would shift the snow zones by 300 m in altitude. Table 1 summarises mean backscatter intensities found on horizontal areas in different snow zones of Northeast Glacier at approximately 68° south (Wunderle 1996b).

4.2 Energy balance model

An energy balance model is used to relate meteorological conditions to the appearance of the snow cover in the ERS-SAR (Schneider *et al.* 1997). The wetness of the snow can be classified from temperature, humidity and radiation recordings. Since any change of weather conditions takes time to be propagated down into deeper layers of the snow not only the meteorological readings at the instant of the satellite's overpass have to be considered but also the time period before image acquisition.

Automatic weather stations (AWS) were operated at three locations on the glaciers marked with crosses in fig. 6a during the summer season 1994/1995 on both glaciers. The data acquired were used to compute sensible heat flux and latent heat flux according to the bulk transfer equations (Brutsaert 1982). The effect of stable stratification in the atmosphere was taken into account using the bulk Richardson number (Ri) and a formulation of the correction term given by Braithwaite (1995). The relation between energy balance estimates and meteorological parameters was further studied using multiple regression analysis in order to derive spatially distributed data. Regression analysis of air temperature and solar irradiance as independent variables and energy balance as dependent variable turned out to be best when performed on the basis of means of six hours or four values per day. Actual temperature gradients calculated from the AWS located at different altitudes were used to provide a spatial data layer of air temperature for each quarter of each day. Short-wave irradiance was modelled employing the Short-Wave-Irradiance-Model (SWIM), described in detail in Parlow (1996). The effect of cloudiness was considered by computing the ratio between modelled and measured irradiance for the three locations of the AWS. Employing an iterative approach this ratio was re-introduced into the modelling scheme of SWIM. Using the coefficients of the multiple regression analysis, the spatial data sets of temperature and irradiance were used to produce estimates of the spatial distribution of the energy balance for each quarter of a day. To separate dry and wet snow zones a simple snow cover model with seven layers of approximately 10 cm depth each was assumed. The idea of the model is to reduce the number of wet layers by one if air temperature and energy budget are negative at a given grid point and to do the opposite if both determining variables show positive values at a grid point. If the snow cover is comprised by only dry layers nothing is changed in case of further cooling. After complete wetting of all seven layers of the upper snow cover this is not enhanced in case of further 'warming'. The snow cover model is optimised according to the local conditions characterised by a snow pack composed of highly metamorphosed snow grains of 1 to 4 mm diameter and interspersed ice lenses. ERS microwave radiation penetrates snow with these properties and with a minimum liquid water content of (0.5%) to a depth of approximately 0.7 m (Friedrich 1996). Therefore we assume that only a model result with all seven layers being completely frozen will result in bright tones on the ERS-1 image as found on the upper parts of McClary glacier. For all grid points with at least one layer containing liquid water a considerable reduction of the backscatter intensity as found on the Northeast glacier on the same frame is predicted.

Fig. 6a represents the status of the model for the time of the satellite's overpass. Contour lines with 100 m intervals are overlaid. The discontinuities in the DTM originate from merging to different DTMs. The transition from wet to frozen percolation zone is modelled correctly for both glaciers. Some discrepancy can be observed to the north of McClary-Glacier. However this may be attributed to inaccuracies of the DTM in this area. The model was also run with data from the summer season 1993/94. During this season mean air temperature was 2.2 K lower than the year later and transition line from wet snow zone to frozen percolation zone was 280 m lower in 1993/1994 than in 1994/95. Model result and SAR images match excellently only for two of the three available images of the 1993/94 summer season (fig. 7). The mismatch of the third image can be attributed to an abrupt weather change a couple of hours before image acquisition. The model overestimates the effect of this sharp rise in temperature.

5. CONCLUSIONS

It is concluded that spaceborne SAR data can be used on the AP to estimate the state of the snow cover. SAR data can be employed to delineate different snow zones. Backscatter from the dry snow zone is generally small because of the small grain sizes. However, it has a considerable contribution from internal strata of the snow pack. Backscatter intensity from snow with large grains below 0°C in the percolation zone is so intense that the contribution of ice lenses only leads to small changes. In the wet snow zone absorption of radiation because of liquid water reduces the backscatter intensity dramatically. Meteorological data and terrain information is useful to reduce ambiguities in the SAR data. On the other hand ERS SAR data helps to obtain spatial evidence of climate variations. Spatial and temporal variations of snow zones can be derived from SAR data. This can also be related to the spatial and temporal variation of climate elements at a regional scale. Therefore spaceborne SAR imagery is a powerful tool for climate monitoring in snow covered regions such as the AP. Spatial estimates of climate variation from remote areas can be obtained, provided that temporal and spatial coverage can be assured for a long sequence of summer seasons.

6. ACKNOWLEDGEMENTS

This research was supported by the German Secretary of Science and Research (BMBF) within the programme 'Dynamic Processes in Antarctic Geosystems' (DYPAG) (Contract Number: 03PL016A) and by the ESA pilot study 'Monitoring Of Dynamic Processes in Antarctic Geosystems' (MODPAG),

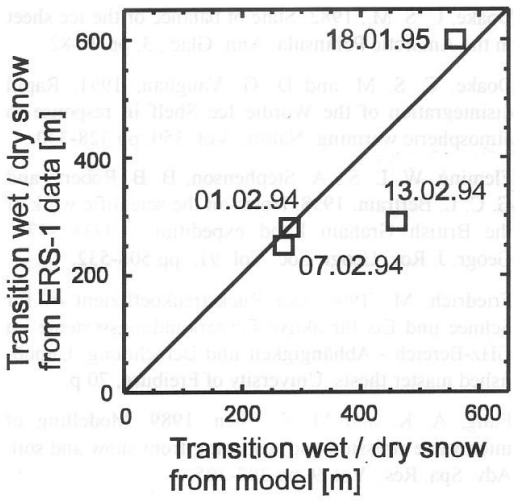

Fig. 7: Average altitude asl of transition from wet to dry snow modelled (x-axis) and derived from ERS-PRI images (y-axis). Due to the small number of ERS frames available, a calculation of correlation was not performed.

(Contract Number: AO2.D149). The authors would like to thank the Instituto Antarctico Argentino (IAA), the British Antarctic Survey (BAS) and the German Alfred-Wegener-Institut für Polar- und Meeresforschung (AWI) for their support in respect to logistics and field equipment during several field campaigns. The authors are grateful for the invaluable assistance and discussions in the field by the Argentine and German collaborators.

7. REFERENCES

Braithwaite, R. J., 1995. Aerodynamic stability and turbulent sensible-heat flux over a melting ice surface, the Greenland ice sheet. J. Glac., Vol. 41, No. 139, pp 562 - 571.

Brutsaert, W., 1982. Evaporation in the Atmosphere. Dortrecht, London, 299 p.

Chuah, H.-T., S. Tjuatja, A. K. Fung and J. W. Bredow, 1997. Radar backscatter from a dense random medium. IEEE Transactions on geoscience and remote sensing, Vol. 35, pp 892-900.

Drinkwater, M. R.,1989. LIMEX '87 Ice surface characteristics: Implications for C-Band SAR backscatter signatures. IEEE Transactions on geoscience and remote sensing, Vol. 27, pp 501-513.

Drinkwater, M. R. and G. B. Crocker, 1988. Modelling changes in the dielectric and scattering properties of young snow-covered sea ice at Ghz frequencies. J. Glac., Vol. 34, pp 274-282.

Doake, C. S. M., 1982. State of balance of the ice sheet in the Antarctic Peninsula. Ann. Glac., 3, pp 77-82.

Doake, C. S. M. and D. G. Vaughan, 1991. Rapid disintegration of the Wordie Ice Shelf in response to atmospheric warming. Nature, Vol. 350, pp 328-330.

Fleming, W. L. S., A. Stephenson, B. B. Roberts and G. C. L. Bertram, 1938. Notes on the scientific work of the British Graham Land expedition. 19934 -37 Geogr. J. Roy. Geogr. Soc. Vol. 91, pp 508-532.

Friedrich, M., 1996. Der Rückstreukoeffizient σ^0 für Schnee und Eis für aktive Fernerkundungssysteme im GHz-Bereich - Abhängigkeit und Berechnung. Unpublished master thesis, University of Freiburg, 70 p.

Fung, A. K. and M. F. Chen, 1989. Modelling of microwave emission and scattering from snow and soil. Adv. Spa. Res., Vol. 9, pp 297-305.

Fung, A. K. and H. J. Eom, 1982. Application of a combined rough surface and volume scattering theory to sea ice and snow backscatter. IEEE Transactions on geoscience and remote sensing, Vol. GE-20, pp 528-535.

Hallikainen, M., 1996. Physical basis for microwave remote sensing of sea ice and snow. in: Raschke, E. (ed.). Radiation and water in the climate system. NATO ASI Series, Springer Verlag, Vol. 145, pp 489 - 525.

Hallikainen, M. T. and F. T. Ulaby, 1986. Dielectric and scattering behaviour of snow at microwave frequencies. Proceedings of IGARSS '86 Symposium, Zürich

Harangozo, S.A., S. R. Colwell and J. C. King, 1997. An analysis of a 34-year air temperature record from Fossil Bluff (71°S, 68°W), Antarctica. Ant. Sci., Vol. 9, pp 355-363.

Houghton, J. T., L. G. Meira Filho, B. A. Callander, N. Harris, A. Kattenberg, K. Maskell, 1996. Climate Change 1995, the science of climate change. IPCC report, Cambridge University Press, Cambridge.

Jezek, K. C. and M. R. Drinkwater *et al.*, 1993. Analysis of synthetic aperture radar data collected over the southwestern Greenland ice sheet,- J. Glac., Vol. 39, pp 119-132.

King, J. C., 1994. Recent climate variability in the vicinity of the Antarctic Peninsula. Int. J. Clim., Vol. 14, pp 357-369.

King J. C. and J. Turner, 1997. Antarctic Meteorology and Climatology. Atmospheric and Space Science Series, Cambridge University Press, Cambridge.

Mätzler, C., 1987. Applications of the interactions of microwaves with the natural snow cover. Rem. Sens. Rev., Vol. 2, pp 259-387.

Morris, E. M. and D. G. Vaughan, 1994. Snow surface temperatures in West Antarctica. Ant. Sci., Vol. 6, pp 529-535.

Oerter, H. 1997. Personal communication. Alfred-Wegener-Institut für Polar-und Meeresforschung, Bremerhaven, Germany.

Parlow, E., 1996. Correction of terrain controlled illumination effects in satellite data. In: Parlow E (ed.). Progress in environmental remote sensing research and applications. Proc. of 15th EARSeL Symp., Basel 04 - 06 Sept. 1995, pp 139 - 145.

Paterson, W. S. B., 1994. The physics of glaciers. 3rd Edition, Elsevier, Kidlington, NewYork.

Peel, D. A., 1992a. Spatial temperature and accumulation rate variations in the Antarctic Peninsula. In: Morris, E. M. (ed.). The contribution of Antarctic Peninsula ice to sea level rise. Brit. Ant. Sur., Ice and Climate Special Report, No. 1, BAS, Cambridge, UK, pp 11-15.

Peel, D. A., 1992b. Ice core evidence from the Antarctic Peninsula region. In: Bradley, R. S. and P. D. Jones (eds.). Climate since A. D. 1400. Routledge, New York, pp 549-571.

Reber, B., C. Mätzler, E. Schanda, 1987. Microwave signatures of snow crusts - Modelling and measurements. Int. J. Rem. Sens., Vol. 8, pp 1649 - 1665.

Reynolds, J. M., 1981. The distribution of mean annual temperatures in the Antarctic Peninsula. Brit. Ant. Sur. Bul., Vol. 54, pp 123-131.

Rott, H. 1984. The analysis of backscattering properties from SAR data of mountain regions. IEEE J. of Oceanic Engeneering, Vol. OE-9, pp 347-355.

Rott, H., P. Skvarca and T. Nagler, 1996. Rapid Collapse of Northern Larsen Ice Shelf. Science, Vol. 271, pp 788-792.

Rott, H. C., K. Sturm and H. Miller, 1993. Active and passive microwave signatures of Antarctic firn by means of field measurements and satellite data. Ann. Glac., Vol. 17, pp 337-343.

Schneider, C., S. Wunderle, H. Gossmann and H. Saurer, 1997. Validation of energy balance estimates from snow covered areas of the Antarctic Peninsula based on ERS-PRI images. Proc. of 3rd ERS Symp., 16. - 21. Apr. 1997, Florence, in print.

Schwerdtfeger, W., 1984. Weather and Climate of the Antarctic. Developments in Atmospheric Science, 15, Elsevier, Amsterdam, New York.

Skvarca, P., 1993. Fast recession of the northern Larsen Ice Shelf monitored by space images. Ann. Glac., Vol. 17, pp 317-321.

Smith, R. C. and S. E. Stammerjohn, 1996. Surface air temperature variations in the western Antarctic Peninsula region. In: Ross, R. M., E. E. Hofmann and L. B. Quetin (eds.). Foundations for Ecological Research West of the Antarctic Peninsula. Ant. Res. Ser., Vol. 70, Amer. Geo. Union, Washington, D.C., pp 105-121.

Stammerjohn, S. E. and R. C. Smith, 1996. Spatial and temporal variability of western Antarctic Peninsula sea ice coverage. In: Ross, R. M., E. E. Hofmann and L. B. Quetin (eds.). Foundations for Ecological Research West of the Antarctic Peninsula, Ant. Res. Ser., Vol. 70, Amer. Geo. Union, Washington, D.C., pp 81-104.

Tiuri, M. E., A. H. Sihvola, E. G. Nyfors and M. T. Hallikainen, 1984. The complex dielectric constant of snow at microwave frequencies. IEEE J. of Oceanic Engeneering, Vol. OE-9, pp 377-382.

Turner, J., S. R. Colwell and S. Harangozo, 1997. Variability of precipitation over the coastal western Antarctic Peninsula from synoptic observations. J. Geophys. Res., Vol. 102, pp 13999-14007.

Ulaby, F. T., F. T. Moore and A. K. Fung, 1986. Microwave remote sensing: Active and passive; Volume III, from theory to applications. Artech House, Norwood, pp 1065 -2162.

Ulaby, F. T., F. T. Moore and A. K. Fung, 1982. Microwave remote sensing: Active and passive; Volume II, radar remote sensing and surface scattering and emission theory. Artech House, Norwood, pp 457 - 1064.

Ulaby, F. T., F. T. Moore and A. K. Fung, 1981. Microwave remote sensing: Active and passive; Volume I, fundamentals and radiometry. Artech House, Norwood, pp 1 - 456.

Vaughan, D. G., 1993. Implications of the break-up of Wordie Ice Shelf, Antarctica for sea level. Ant. Sci., Vol. 5, pp 403-408.

Vaughan D. G. and C. S. M. Doake, 1996. Recent atmospheric warming and retreat of ice shelves on the Antarctic Peninsula. Nature, Vol. 379, pp 328 - 330.

West, R., L. Tsang and D. P. Winebrenner 1993. Dense medium radiative transfer theory for two scattering layers with a Rayleigh distribution of particle sizes. IEEE Transactions on geoscience and remote sensing, Vol. 31, pp 426-437.

West, R. *et al.* 1996. Microwave emission from density-stratified Antarctic firn at 6 cm Wavelength. J. Glac., Vol. 42, pp 63-.

Wunderle S., 1996a. A comparison between the dry snow lines derived from meteorological data and ERS-1 SAR images on the Antarctic Peninsula. In: Parlow E. (ed.). Progress in environmental remote sensing research and applications. Proc. of 15th EARSeL Symp., Basel 04 - 06 Sept. 1995, pp 249 - 252.

Wunderle S., 1996b. Die Schneedeckendynamik der Antarktischen Halbinsel und ihre Erfassung mit aktiven und passiven Fernerkundungsverfahren. Freiburger Geographische Hefte. Nr. 48, University of Freiburg, 172 p.

Wunderle, S. and H. Saurer, 1995. Snow properties of the antarctic peninsula derived from ERS-1 SAR images. Proc. of the 21st Ann. Conf. of the Rem. Sens. Soc., 11.-14. Sept. 1995, Uni. of Southampton, pp 1231-1237.

Wyeth, R. B., 1977. The physiography and significance of the transition zone between Graham Land and Palmer Land. Brit. Ant. Sur. Bul., Vol. 46, pp 39-58.

Zwally, H. J. and S. Fiegles, 1994. Extent and duration of Antarctic surface melting. J. Glac., Vol. 40, pp 463-476.

Zwally, H. J., C. L. Parkinson and J. C. Comiso, 1983. Variability of Antarctic Sea Ice and Changes in Carbon Dioxide. Science, Vol. 220, pp 1005-1012.